eXPRESS Polymer Letters Vol.3, No.10 (2009) 621–629
Available online at www.expresspolymlett.com
DOI: 10.3144/expresspolymlett.2009.78

Scratch resistance of a polycarbonate + organoclay nanohybrid

A. Arribas[1], *M.-D. Bermúdez*[2], *W. Brostow*[3,*], *F. J. Carrión-Vilches*[2,3], *O. Olea-Mejía*[3,4]

[1]Centro Tecnológico del Calzado y Plástico de la Región de Murcia, Polígono Industrial Las Salinas, Avda. Europa 4-5, 30840 Alhama de Murcia, Spain
[2]Grupo de Ciencia de Materiales e Ingeniería Metalúrgica, Departamento de Ingeniería de Materiales y Fabricación, Universidad Politécnica de Cartagena, Campus de la Muralla del Mar, C/ Doctor Fleming s/n, 30202 Cartagena, Spain
[3]Laboratory of Advanced Polymers & Optimized Materials (LAPOM), Department of Materials Science & Engineering, University of North Texas, 1150 Union Circle # 305310, Denton, TX 76203-5017, USA
[4]Centro de Investigación en Química Sustentable (CIQS), Facultad de Química, Universidad Autónoma del Estado de México, Km. 12 de la carretera Toluca-Atlacomulco, San Cayetano, C.P. 50120, Mexico

Received 17 March 2009; accepted in revised form 10 July 2009

Abstract. A polycarbonate-based nanohybrid has been created containing 1 wt% of Bentone 2010, an organically modified montmorillonite. A micro-section on the nanohybrid obtained using focused ion beam (FIB) and field emission scanning electron microscopy (FESEM) was employed to observe the orientation of the nanoclay inside a polycarbonate (PC) matrix in the cross-section FIB-milled face. A micro-scratch tester was used to measure the scratch resistance in terms of residual (healing) depth R_h under progressive load and in sliding wear. Effects of the number of scratches, normal load and scratch velocity have been evaluated as a function of nanoclay orientation. In sliding wear (multiple scratching along the same groove), our nanohybrid reaches residual depth values that remain constant after a certain number of scratches, a manifestation of strain hardening. The number of scratches to induce strain hardening decreases as the normal applied load increases. SEM was used to characterize deformation and wear mechanisms that operate on contacts and the results related to the wear data.

Keywords: *nanocomposites, polycarbonate, FIB, scratch resistance, wear resistance*

1. Introduction

There exists a belief that addition of nanoparticles to polymers results in improvement of a variety of properties of the matrix polymer. This statement is not always true. Thus, for epoxy + silica nanohybrids there is an improvement of both mechanical and tribological properties [1]. By contrast, for Polyamide 6 reinforced with multiwall carbon nanotubes (MWCNTs) there is an improvement of mechanical properties; however, scratch recovery is hampered by the presence of CNTs [2] while the scratch depths can be either shallower or deeper, depending on the CNTs diameter and also on functionalization. Thus, creation of polymer-based nanohybrids seems be a two-edged sword.

Fairly large amount of work has been expended on organoclay-containing hybrids. Thus, Xu *et al.* [3] have created such hybrids on the basis of thermoplastic polyurethanes (TPUs) and investigated their tribological behavior against steel. The presence of organoclay has improved resistance to rolling wear significantly. Dynamic friction decreased for TPUs with low hardness but increased for TPUs with high hardness – hence also here we are dealing with

*Corresponding author, e-mail: wbrostow@yahoo.com

a two-edged sword. In general, tribology of polymer-based materials (PBMs) is significantly more difficult than tribology of metals although some approaches that work have been developed [4–20]. In this situation, we have decided to investigate further effects of the presence of organoclay on tribological behavior an engineering polymer. In an earlier paper [13] some of us have demonstrated using transmission electron microscopy [TEM] that there is a preferential orientation of nanoclay in the polymer matrix. Apparently the orientation appears during the injection molding process due to high shear pressure in the melt.

2. Experimental

2.1. Materials

PC and PC + 1 wt% B2010 were prepared using Lexan LS2 from General Electric Plastics and Bentone 2010 (B2010), a quaternary ammonium-modified montmorillonite that was supplied by Elementis Specialties, and used as received. After mixing in the corresponding proportion, extrusion and injection molding were carried out to obtain samples of PC and PC + 1% B2010 as previously described [13].

2.2. Thermophysical properties

Differential scanning calorimetry (DSC) was performed using a Mettler Toledo DSC 822. Samples of 9.78 mg for PC and 14.01 mg for PC + 1% B2010 were heated above the glass transition temperature T_g, then kept at 300°C for 5 minutes, cooled, and a second heating run was made between 0 and 300°C at the heating rate of 20°C/min in nitrogen atmosphere, with the flow rate of 50 ml/min. Thermogravimetric analysis (TGA) to determine degradation temperatures T_d was carried out using a Mettler Toledo TGA SDTA 851 analyzer at the heating rate of 20°C/min from 30 to 950°C in an oxygen flow of 40 ml/min.

2.3. Hardness measurement

Hardness values were determined with a TH210 Shore D hardness tester.

2.4. Focused Ion Beam (FIB) & Field Emission Scanning Electron Microscopy (FESEM)

A FEI Nova 200 Dual Beam consisting of FIB and FESEM was used to obtain cross-sections of the materials in order to evaluate the dispersion, distribution and orientation of the nanoclay in relation to the melt flow direction during the process of the injection molding. The equipment combination was the same as used in earlier work [14], the source consisted of gallium ions. We have cut with FIB precise micro-sections before FESEM. The conditions of the micro-sectioning were 17 nA probe current and 15.0 kV accelerating voltage. The micro-sections with dimensions of 6.0×5.0×5.0 μm took 20 minutes at 52° of tilt, followed by 2 cycles of cleaning for 40 s.

2.5. Scratch testing

Specimens were tested using a CSM Micro-Scratch Tester (MST) following the procedure previously described [1, 2, 6, 15–17]. Sliding wear (repetitive scratching along the same groove) tests were performed as follows: normal load 5.0, 10.0 and 15.0 N; scratch length 5.0 mm; scratch velocity 2.5, 5.0 and 15.0 mm/min at room temperature. In progressive scratch testing, progressively increasing loads from 0.03 to 30.0 N were applied at 5.0 N/min rate along 5.0 mm of length. A conical diamond indenter was used in all the tests with the diameter of 200 μm and a cone angle of 120°. The results include the penetration (instantaneous) depth R_p and the residual (healing) depth R_h. Following the scratch test and a waiting period of 2 minutes to allow for viscoelastic recovery, the indentor makes a scan along the track scratch at 0.03 N contact load to determinate the residual depth. Repeated experiments have confirmed that the shallower residual depth in our viscoelastic materials is reached inside 2 minutes. Therefore, R_h values have in each case been determined 5 minutes after recording the R_p values.

2.6. Scanning electron microscopy (SEM)

SEM images of the scratch track were obtained using a Hitachi S3500 N scanning electron microscope. The samples were sputter coated with a thin

layer of gold in order to make them conductive with the aid of a SC7640 Sputter Coater from Polaron.

3. Hardness and thermophysical properties

Table 1 shows hardness values and thermophysical properties of the materials. Hardness values are very similar for both materials. The addition of 1 wt% B2010 increases thermal stability of PC, as can be seen by the degradation temperatures. Nanoclay layers provide a barrier action against heat diffusion – what improves the thermal stability of the nanohybrid [21].

The glass transition temperature decrease shows that nanoclay acts as a plasticizer of PC. Apparently, nanoclay particles increase the mobility of PC chains. In more detail: when a sequence of chain segments 'would like' to move, the surrounding chains form a barrier to the movement because of entanglements – a fact pointed out by Treloar long ago [22]. However, if the nearest environment of that sequence consists of clay particles, those particles can move away since there are no such constraints.

Figures 1a and 1b display FESEM images of the nanohybrid where the nanoclay platelets are largely aligned parallel (*L*) to the melt flow direction [23–25]. The observed orientation could be the result of the response of the nanoclay layers to high shear forces applied during the extrusion and injection of the specimen. In the following sections, the scratching resistance of the nanohybrid will be discussed in the longitudinal (*L*) direction parallel to the melt flow and in the transverse (*T*) direction perpendicular to the melt flow (Figure 1b). An energy-dispersive X-ray spectrum (EDS) of the nanoclay (Figure 1c) confirms the presence of the filler.

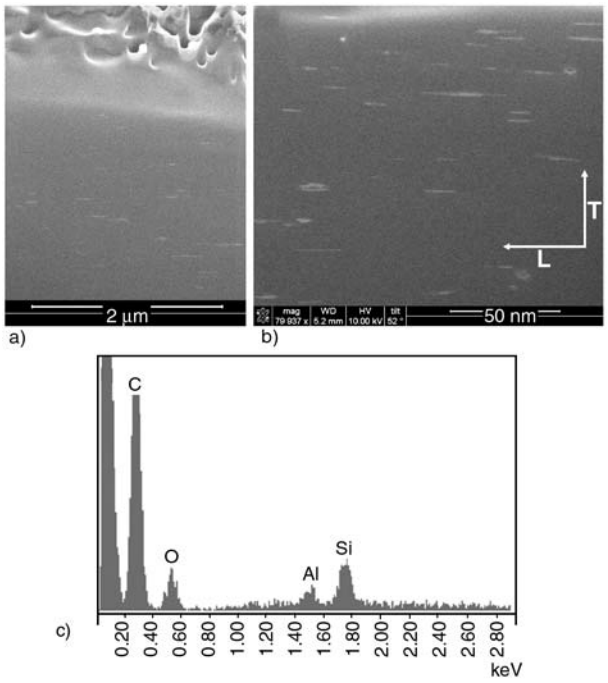

Figure 1. a) Image of Field Emission Scanning Electron Microscopy of a milled micro-section of PC + 1% B2010 using FIB technique; b) magnification of 1a showing longitudinal (*L*) and transverse (*T*) sliding directions with respect to nanoclay orientation; c) energy-dispersive X-ray spectrum (EDS) of the nanoclay

4. Scratching and sliding wear results

4.1. Progressive scratch testing

As discussed in an earlier paper [13], we have undertaken a study of the influence of nanoclay orientation when the sliding direction is either longitudinal (*L*) or transverse (*T*) to the orientation of the nanoclay (see Figure 1b). Figure 2 shows residual depth values as a function of scratch direction. A linear response to increased applied load is observed in all cases. In the longitudinal direction (Figure 2a), nanoclay reduces R_h with respect to neat PC, while R_h values are similar for both materials in the transverse direction (Figure 2b). For an explanation see the discussion of plasticizing behavior of nanoclay particles above in Section 3.

If we consider the reduction of R_h with load for the nanohybrid with respect to PC in the longitudinal direction (Figure 2c), we can fit the results to an exponential decay function (Equation (1)):

$$R_h \text{ reduction } [\%] = 10.64 + 61.10 \cdot e^{(-0.21 \cdot \text{Load})} \quad (1)$$

with good accuracy (the parameter $R = 0.983$). Thus, the presence of the nanoclay reinforcement is

Table 1. Hardness and thermal properties of the materials

Material	Hardness Shore D	T_g [°C]	T_d [°C]			
			1st step		2nd step	
			Onset	Midpoint	Onset	Midpoint
PC	81.3	145.1	475	504	552	565
PC + 1% B2010	81.8	133.6	494	510	572	608

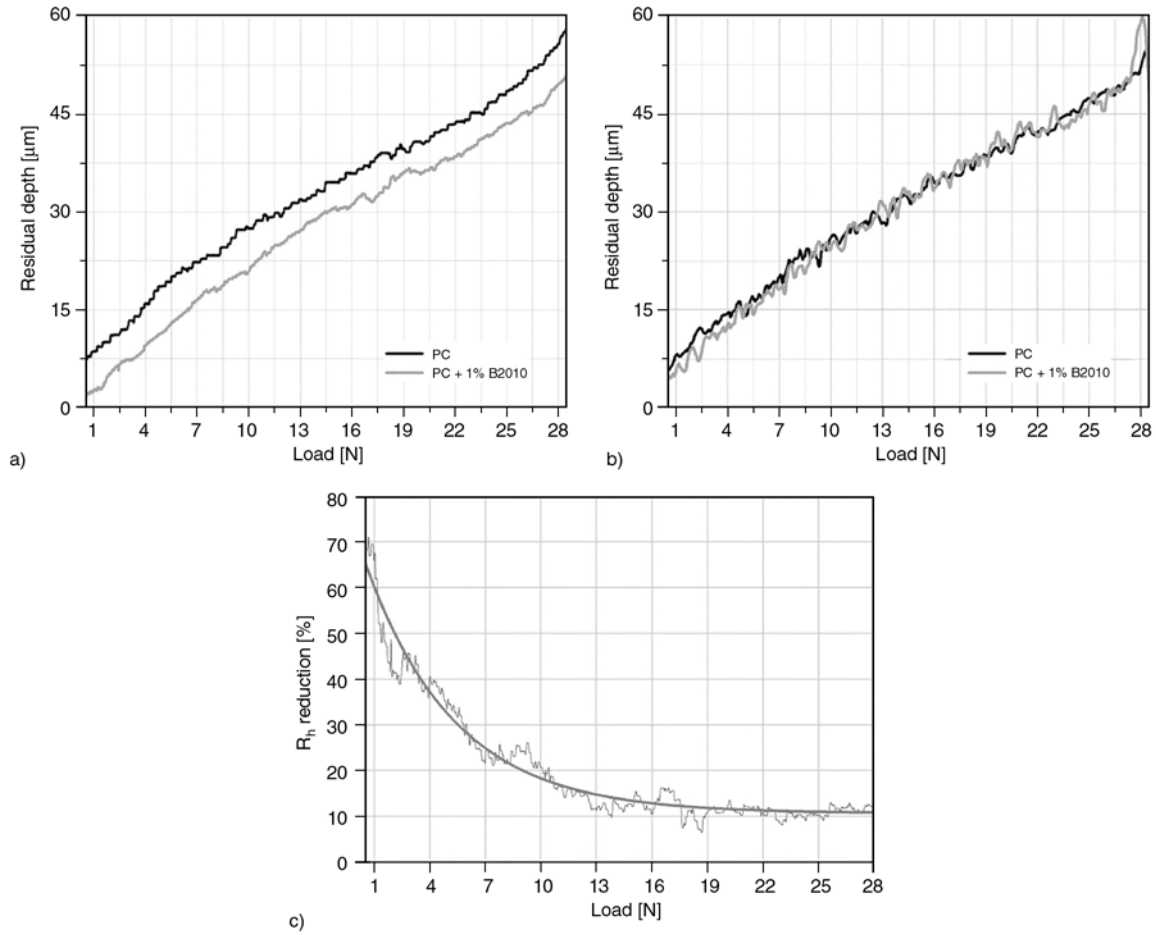

Figure 2. Residual depth under progressive load tests for PC and PC + 1% B2010 as a function of scratch direction: a) longitudinal; b) transverse; c) R_h reduction with load for the composite with respect to PC in the longitudinal direction

less effective as the applied load increases. Apparently, the first nanoclay particles put in have a larger effect on the mobility of macromolecular chains than the subsequent ones. The absence of slope changes in the R_h vs. load graphs in Figure 2a and 2b suggests that no fracture takes place during the progressive load tests.

Figure 3 shows the SEM micrographs of the tracks on neat PC (Figure 3a and 3c) and on the nanohybrid (Figure 3b and 3d), both in longitudinal and transverse directions. In the case of PC in the transverse direction (Figure 3c), we observe the presence of regular cracks inside the scratch groove. The cracks follow the original surface texture; we observe the presence of wear debris particles inside the groove in the longitudinal direction (Figures 3a and 3b). There is less damage on the surface of the composite as compared to neat PC. Apparently nanoclay helps to dissipate the stress during contact with the indenter.

Results of computer simulation of scratch testing using the molecular dynamics method [8] have been reported. However, results so far available pertain to neat polymers only.

4.2. Sliding wear

We have previously reported [17, 26] that glassy polystyrene (PS) is an exception among all polymers investigated in sliding wear mode. Namely, PS does not show a horizontal asymptote in residual depth values as a function of the number of scratches. In other words, in the case of PS, there is no strain hardening in multiple sliding along the same groove. This finding has led us to the definition of brittleness [27, 28].

However, as we have shown earlier [15], addition of 1 wt% of a liquid-crystalline additive induced the strain hardening effect in PS. This has led us to the idea to determine the sliding wear resistance of

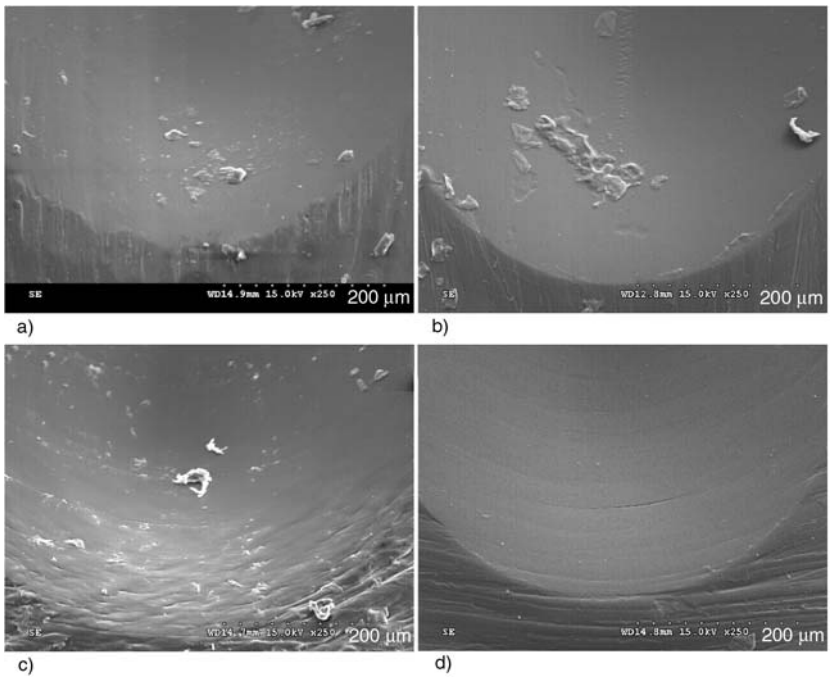

Figure 3. SEM micrographs after progressive load testing: a) PC in the longitudinal direction; b) composite in the longitudinal direction; c) PC in the transverse direction and d) composite in the transverse direction

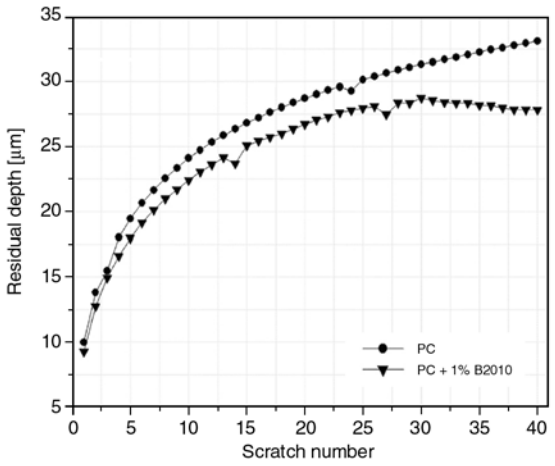

Figure 4. Residual depth under multiscratching for PC and PC + 1% B2010 in the transverse direction

PC (another glassy polymer) and effects of the nanoclay additive.

The tests were performed along the transverse direction with respect to the melt flow, perpendicular to nanoclay orientation (see again Figure 1b) that gave similar results for PC and the nanohybrid under the progressive load testing (Figure 2b).

Figure 4 shows the residual depth values for PC and the nanohybrid after 40 scratches. The higher scratch resistance of the hybrid is evident from the initial scratches and increases as the number of scratches increases. After 22 or so scratches we see a difference between PC and the nanohybrid. We see strain hardening (originally discovered in [16])

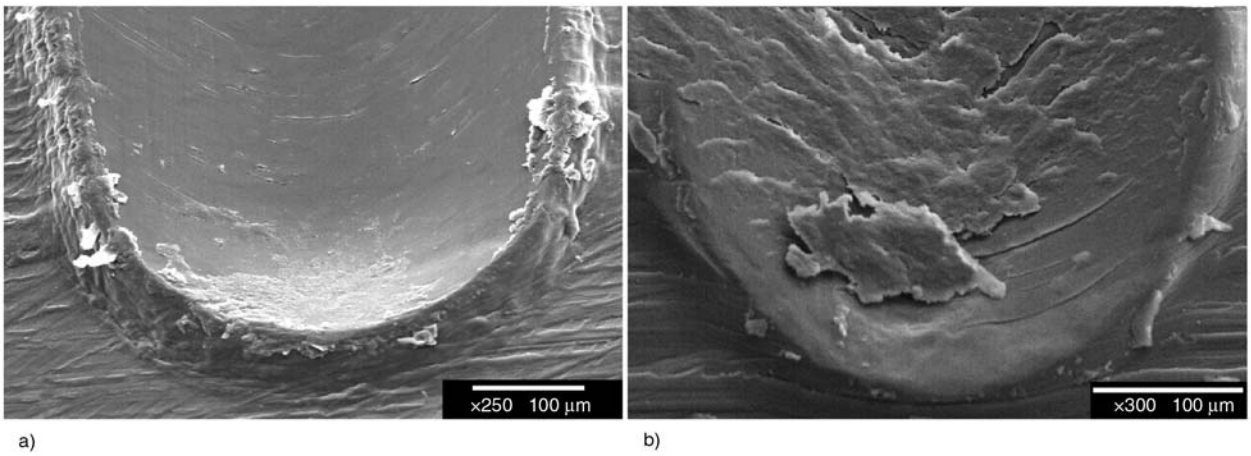

Figure 5. SEM micrographs after 40 scratches of: a) PC; b) PC + 1% B2010

in the hybrid – clearly due to the presence of nanoclay – but not in neat PC.

Scratch grooves of both materials are seen in SEM (Figure 5). PC (Figure 5a) shows a flat and smooth surface, with the presence of periodic cracks perpendicular to the sliding direction, and accumulation of plastically deformed material at the edges of the track. The nanohybrid (Figure 5b) shows a scratch groove covered by a layer of plastically deformed material. The better performance of the nanohybrid can be attributed to the stability of the plastically deformed layer.

Figure 6 displays diagrams of the residual depth R_h under variable load as a function of the scratch number and sliding direction for PC (Figure 6a) and for the nanohybrid (Figure 6b). For PC we see R_h nearly independent of the sliding direction. As anticipated by Figure 4, strain hardening is seen in the nanohybrid.

Under low load of 5.0 N, the sliding wear resistance of the nanohybrid is independent of the scratch direction. Under 10.0 N, a higher resistance in the transverse direction is observed, with a maximum R_h reduction of 26.8% for the transverse direction (T-10N; Figure 6b) with respect to the longitudinal one (L-10N; Figure 6b).

We note that the nanohybrid shows the strain hardening effect (with constant or slightly decreasing R_h values) after 12 scratches, under 15.0 N in the

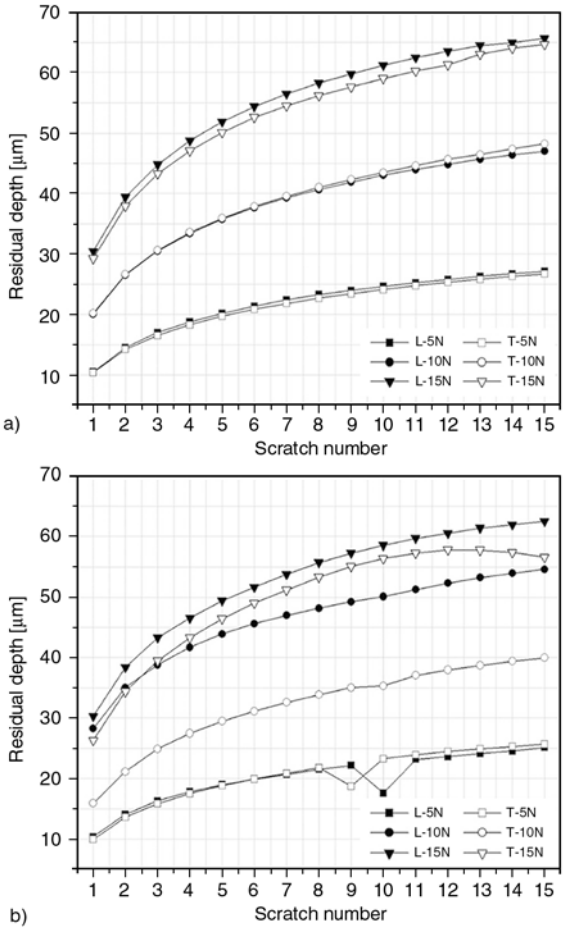

Figure 6. Residual depth under multiscratching as a function of normal load and direction: a) PC; b) nanohybrid

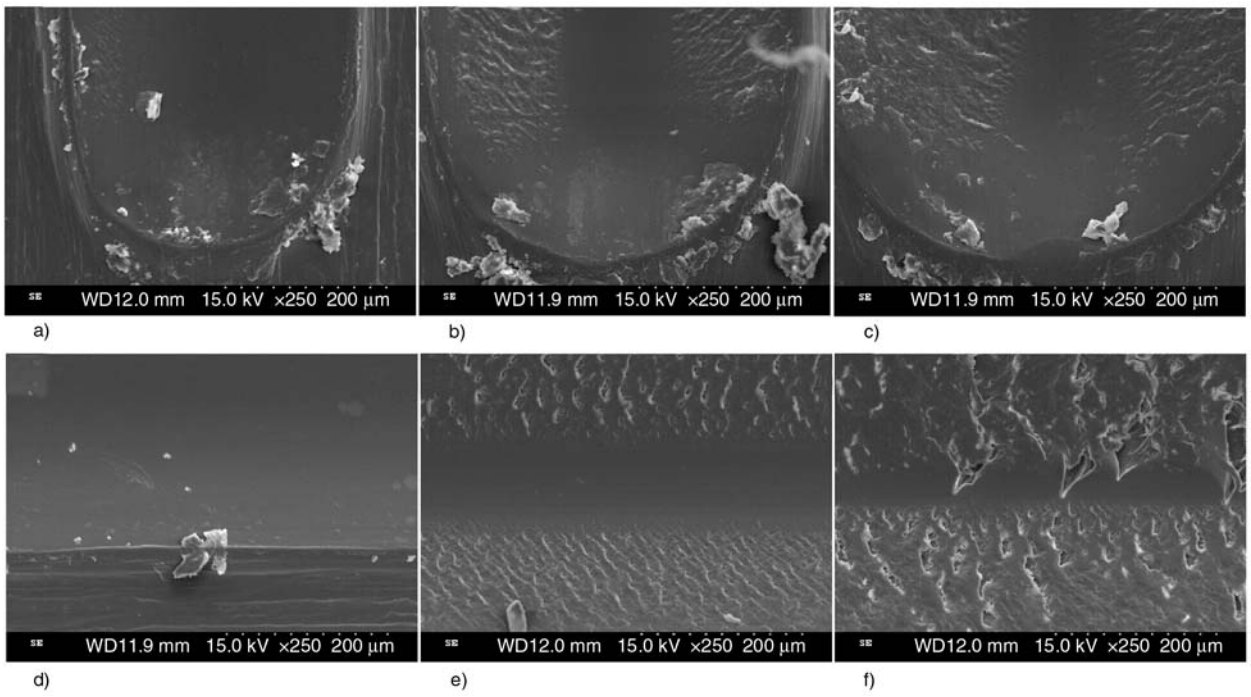

Figure 7. SEM images and magnifications of the nanohybrid scratch grooves in the longitudinal direction: a) and d) 5.0 N; b) and e) 10.0 N; c) and f) 15.0 N

transverse direction (T-15N in Figure 6b). This behavior is similar to that seen after 27 scratches under the normal load of 5.0 N in the transverse direction (Figure 4). It can be concluded that the number of scratches to induce strain hardening decreases as the applied normal load increases.

SEM images in Figure 7 show the severity of the nanohybrid surface damage as a function of the normal load after 15 scratches in the longitudinal direction. Images at the top (a–c) were taken along the scratches, images at the top (d–f) across the scratches. Under 5.0 N (Figures 7a and 7d), a mild plastic deformation and a smooth surface is observed. When the normal load applied is increased to 10.0 N (Figures 7b and 7e) a crazing mechanism with the presence of cracks at the edges of the scar and finally, under 15.0 N, severe plastic deformation and large cracks appear (Figures 7b and 7c).

4.3. Effects of scratch velocity

Variable scratching velocity tests were carried out under the normal load of 5.0 N. Figure 8 shows the change of R_h as a function of scratch number obtained for three velocities on PC (Figure 8a) and the nanohybrid (Figure 8b) in both longitudinal and transverse directions. In the case of PC (Figure 8a), R_h decreases under increasing velocity. A possible explanation is that, at higher velocity, the indenter damages a smaller number of specific locations [26]. Another explanation is that mechanical damage is the main mechanism at low velocities, an effect weakened by thermally induced deformations at high velocities [9, 10]. In this context, heat dissipation at higher velocities necessarily increases free volume v_f. In turn, higher v_f enhances the chain relaxation capability (CRC) and thus viscoelastic recovery [29–31]. Both explanations might be true simultaneously.

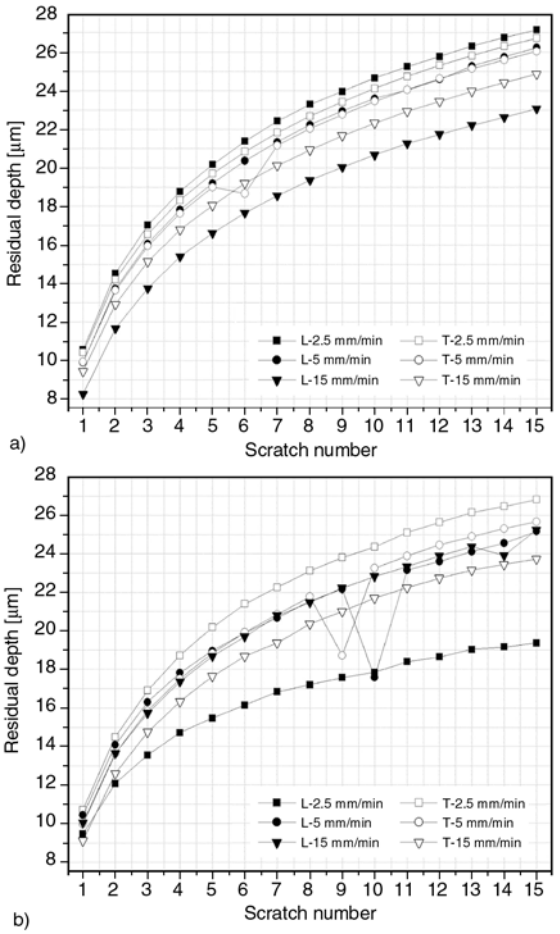

Figure 8. Residual depth in sliding wear determination as a function of scratch velocity and direction: a) PC; b) nanohybrid

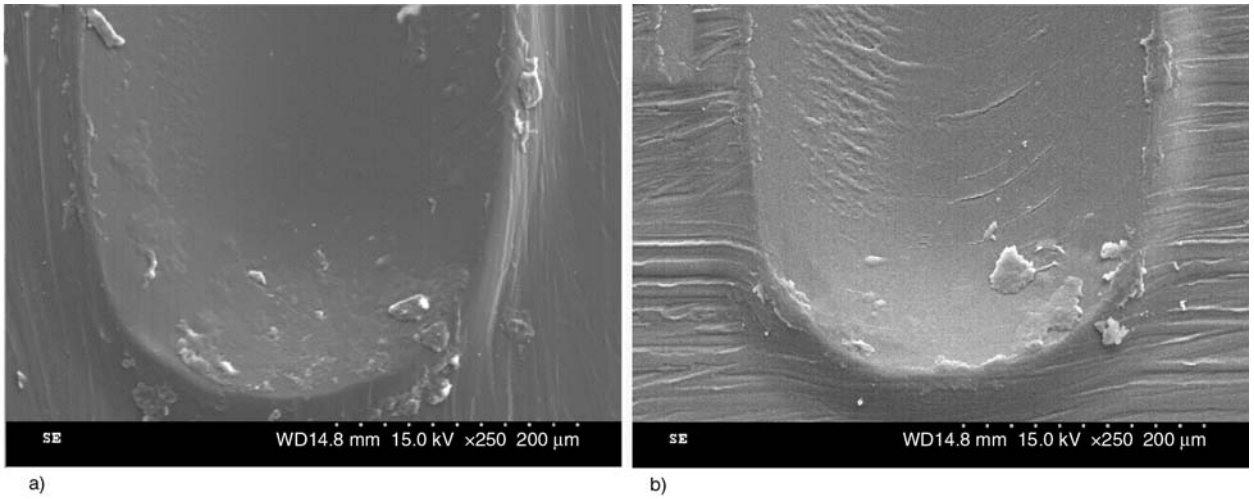

Figure 9. SEM images for the nanohybrid at 2.5 mm/min as a function of the scratch direction: a) longitudinal; b) transverse

The nanohybrid shows an R_h decrease under increasing velocity only in the transverse direction. By contrast, in the longitudinal direction the minimum R_h values are found at the lowest scratch velocity (L-2.5 mm/min; Figure 8b), that is a 27.7% reduction in R_h with respect to the transverse direction (T-2.5 mm/min; Figure 8b). We infer that in the longitudinal direction neither the mechanism of less contacts at higher velocities nor the higher heat dissipation at higher velocities are operative. The maximum R_h reduction of 28.6% is obtained for the nanohybrid with respect to PC at the lowest velocity, L-2.5 mm/minute.

Figure 9 illustrates various wear mechanisms in the nanohybrid. There is a small quantity of debris particles formed in the longitudinal direction (Figure 9a) and crack initiation in the transverse direction (Figure 9b).

A question was asked: are nanocomposites any good for anything? In [13] we have found that pin-on-disk friction of polycarbonate is lowered by addition of the nanoclay. Similar friction lowering was achieved by addition of silica nanoparticles to a commercial epoxy [1]. Carbon nanotubes lower the residual depth of Polyamide 6 in sliding wear determination [32]. Windle and his colleagues report 'a variety of effects' in poly(ether ether ketone) (PEEK) + carbon nanofibers systems, but in particular a reduction of wear rate of PEEK [33]. These results are significant since nanocomposites are mostly made to improve mechanical properties rather than tribological ones. We have already noted in the Introduction that going from a neat polymer to a nanohybrid seems a two-edged sword. Thus, nanofillers in polymers can be useful but there are not panacea.

Acknowledgements

We would like to thank the Ministerio de Ciencia e Innovación, Madrid, and Programa de Generación de Conocimiento Científico de Excelencia de la Fundación Séneca, Agencia de Ciencia y Tecnología de la Región de Murcia (Grant # II PCTRM 2007-10), for financial support of the projects MAT2008-01670/MAT and 08596/PI/08, respectively. Francisco J. Carrión-Vilches is grateful to Fundación Séneca for a grant under the program 'Estancias Externas de Investigadores de la Región de Murcia'. Financial support of this work by the Hispanic and Global Studies Initiatives Fund of the University of North Texas, Denton, and the Robert A. Welch Foundation, Houston (Grant # B-1203) are acknowledged also. Discussions with Dr. Nicholas Randall, CSM Instruments, Needham, MA, are appreciated.

References

[1] Brostow W., Chonkaew W., Datashvili T., Menard K. P.: Tribological properties of epoxy+silica hybrid materials. Journal of Nanoscience and Nanotechnology, **9**, 1916–1922 (2009). DOI: 10.1166/jnn.2009.368

[2] Giraldo L. F., Brostow W., Devaux E., López B. L., Pérez L. D., León D.: Scratch and wear resistance of Polyamide 6 reinforced with multiwall carbon nanotubes. Journal of Nanoscience and Nanotechnology, **8**, 3176–3183 (2008). DOI: 10.1166/jnn.2008.092

[3] Xu D., Karger-Kocsis J., Schlarb A. K.: Rolling friction and wear of organoclay-modified thermoplastic polyurethane rubbers against steel. Kautschuk, Gummi, Kunststoffe, **61**, 98–106 (2008).

[4] Steijn R. P.: Friction and wear in: 'Failure of plastics' (eds.: Brostow W., Corneliussen R. D.) Hanser, New York, 356–392 (1986).

[5] Rabinowicz E.: Friction and wear of materials. Wiley, New York (1995).

[6] Brostow W., Deborde J-L., Jaklewicz M., Olszynski P.: Tribology with emphasis on polymers: Friction, scratch resistance and wear. Journal of Materials Education, **24**, 119–132 (2003).

[7] Myshkin N. K., Petrokovets M. I., Kovalev A. V.: Tribology of polymers: Adhesion friction, wear and mass-transfer. Tribology International, **38**, 910–921 (2005). DOI: 10.1016/j.triboint.2005.07.016

[8] Brostow W., Hinze A. J., Simões R.: Tribological behavior of polymers simulated by molecular dynamics. Journal of Materials Research, **19**, 851–856 (2004). DOI: 10.1557/JMR.2004.0110

[9] Felhős D., Xu D., Schlarb A. K., Váradi K., Goda T.: Viscoelastic characterization of an EPDM rubber and finite element simulation of its dry rolling friction. Express Polymer Letters, **2**, 157–164 (2008). DOI: 10.3144/expresspolymlett.2008.21

[10] Karger-Kocsis J., Felhős D., Bárány T., Czigány T.: Hybrids of HNBR and in situ polymerizable cyclic butylene terephthalate (CBT) oligomers: Properties and dry sliding behaviour. Express Polymer Letters, **2**, 520–527 (2008). DOI: 10.3144/expresspolymlett.2008.62

[11] Karger-Kocsis J., Felhős D., Xu D., Schlarb A. K.: Unlubricated sliding and rolling wear of thermoplastic dynamic vulcanizates (Santoprene) against steel. Wear, **265**, 292–300 (2008). DOI: 10.1016/j.wear.2007.10.010

[12] Khan M. S., Lehmann D., Heinrich G., Gohs U., Franke R.: Structure-property effects on mechanical, friction and wear properties of electron modified PTFE filled EPDM composite. Express Polymer Letters, **3**, 39–48 (2009).
DOI: 10.3144/expresspolymlett.2009.7

[13] Carrión F. J., Arribas A., Bermúdez M-D., Guillamon A.: Physical and tribological properties of a new polycarbonate-organoclay nanocomposite. European Polymer Journal, **44**, 968–977 (2008).
DOI: 10.1016/j.eurpolymj.2008.01.038

[14] Brostow W., Gorman B. P., Olea-Mejia O.: Focused ion beam milling and scanning electron microscopy characterization of polymer+metal hybrids. Materials Letters, **61**, 1333–1336 (2007).
DOI: 10.1016/j.matlet.2006.07.026

[15] Bermúdez M. D., Brostow W., Carrión-Vilches F. J., Cervantes J. J., Pietkiewicz D.: Friction and multiple scratch behavior of polymer+monomer liquid crystals systems. Polymer, **46**, 347–462 (2005).
DOI: 10.1016/j.polymer.2004.11.003

[16] Brostow W., Darmarla G., Howe J., Pietkiewicz D.: Determination of wear of surfaces by scratch testing. e-Polymers, no. 025 (2004).

[17] Bermúdez M-D., Brostow W., Carrión-Vilches F. J., Cervantes J. J., Pietkiewicz D.: Wear of thermoplastics determined by multiple scratching. e-Polymers, no. 001 (2005).

[18] Brocka Z., Schmachtenberg E., Ehrenstein G. W.: Radiation crosslinking engineering thermoplastics for tribological applications. in 'Proceedings of Annual Technical Conference of the Society of Plastics Engineers (SPE ANTEC) Cincinnati, USA' 1690–1694 (2007).

[19] Bismarck A., Brostow W., Chiu R., Hagg Lobland H. E., Ho K. K. C.: Effects of surface plasma treatment on tribology of thermoplastic polymers. Polymer Engineering and Science, **48**, 1971–1976 (2008).
DOI: 10.1002/pen.21103

[20] Brostow W., Buchman A., Buchman E., Olea-Mejia O.: Polymer matrix+metal powder microhybrids. Polymer Engineering and Science, **48**, 1977–1981 (2008).
DOI: 10.1002/pen.21119

[21] Valera-Zaragoza M., Ramírez-Vargas E., Medellín-Rodríguez F. J., Huerta-Martínez B. M.: Thermal stability and flammability properties of heterophasic PP-EP/EVA/organoclay nanocomposites. Polymer Degradation and Stability, **91**, 1319–1325 (2006).
DOI: 10.1016/j.polymdegradstab.2005.08.011

[22] Treloar R. L. G.: The physics of rubber elasticity. Clarendon Press, Oxford (1975).

[23] Yuan M., Song Q., Turng L-S.: Spatial orientation of nanoclay and crystallite in microcellular injection molded polyamide-6 nanocomposites. Polymer Engineering and Science, **47**, 765–779 (2007).
DOI: 10.1002/pen.20752

[24] Yuan M., Turng L. S.: Microstructure and mechanical properties of microcellular injection molded polyamide-6 nanocomposites. Polymer, **47**, 7273–7292 (2005).
DOI: 10.1016/j.polymer.2005.06.054

[25] Wang K., Zhao P., Yang S., Liang S., Zhang Q., Du R., Fu Q., Yu Z., Chen E.: Unique clay orientation in the injection-molded bar of isotactic polypropylene/clay nanocomposite. Polymer, **47**, 7103–7110 (2002).
DOI: 10.1016/j.polymer.2006.08.022

[26] Bermúdez M.-D., Brostow W., Carrión-Vilches F. J., Cervantes J. J., Damarla G., Perez J. M.: Scratch velocity and wear resistance. e-Polymers, no. 003 (2005).

[27] Brostow W., Hagg Lobland H. E., Narkis M.: Sliding wear, viscoelasticity and brittleness of polymers. Journal of Materials Research, **21**, 2422–2428 (2006).
DOI: 10.1557/JMR.2006.0300

[28] Brostow W., Hagg Lobland H. E.: Predicting wear from mechanical properties of thermoplastic polymers. Polymer Engineering and Science, **48**, 1982–1985 (2008).
DOI: 10.1002/pen.21045

[29] Brostow W.: Performance of plastics. Hanser, Munich (2000).

[30] Goldman A. Y.: Viscoelasticity, creep and stress relaxation. in 'Performance of plastics' (ed.: Brostow W.) Hanser, Munich 121–146 (2000).

[31] Brostow W.: Reliability and prediction of long term performance of polymer-based materials. Pure and Applied Chemistry, **81**, 417–432 (2009).
DOI: 10.1351/PAC-CON-08-08-03

[32] Giraldo L. F., López B. L., Brostow W.: Effects of the type of carbon nanotubes on tribological properties of Polyamide 6. Polymer Engineering and Science, **49**, 896–902 (2009).
DOI: 10.1002/pen.21386

[33] Werner P., Alstädt V., Jaskulka R., Jacobs O., Sandler J. K. W., Shaffer M. S. P., Windle A. H.: Tribological behaviour of carbon-nanofibre-reinforced poly(ether ether ketone). Wear, **257**, 1006–1014 (2004).
DOI: 10.1016/j.wear.2004.07.010